

Synchronization of propagating spin waves in spin Hall oscillators: A micromagnetic study

Synchronization of propagating spin waves in spin Hall oscillators: A micromagnetic study

Mohammad Haidar

Department of Physics, American University of Beirut, Riad El-Solh,, Beirut, 1107-2020, Lebanon^{a)}

(Dated: 10 March 2025)

In this study, we investigate the synchronization of propagating spin waves in a novel spin torque oscillator device layout using micromagnetic simulations. This design enables individual probing of the dc current in each oscillator, allowing precise control over the synchronization state and providing direct phase measurement. Our findings reveal that two adjacent oscillators achieve phase locking when they maintain a constant phase difference, either in phase or anti-phase, depending on their separation distance. This work offers new insights into STO synchronization mechanisms and paves the way for improved control and functionality in spintronic devices.

arXiv:2503.05391v1 [cond-mat.mtrl-sci] 7 Mar 2025

^{a)}Electronic mail: mh280@aub.edu.lb

I. INTRODUCTION

The synchronization of oscillatory systems is a fundamental phenomenon observed in nature, where mutual interactions among oscillators lead to a collective rhythm¹. In the field of spintronics, spin torque oscillators (STOs) have emerged as a versatile platform for studying nonlinear dynamics and exploring practical applications, such as microwave signal generation^{2–6}, neuromorphic computing^{7–9}, and wireless communication¹⁰. Synchronization among spin-torque oscillators is a particularly intriguing phenomenon, as it enhances their output power, spectral purity, and coherence^{11–14}. Various coupling mechanisms, including magnetic dipolar interactions^{15–17}, spin waves^{18–21}, and electrical coupling^{22,23}, have been explored to achieve both short- and long-range synchronization. Additionally, advances in the long-range synchronization of spin-torque oscillators using spin waves have opened doors for creating highly interconnected oscillator networks with applications in complex problem-solving, such as Ising machines^{24,25}. Among different layout of oscillators, the spin Hall nano-oscillators (SHNOs), a new class of oscillators consisting of a ferromagnet/heavy metal (FM/HM) bilayer, are promising candidates for synchronization in one- and two-dimensional arrays^{26,27}. However, in these devices, synchronization is dictated by dipolar fields. With the recent development of SHNOs and including perpendicular magnetic anisotropy (PMA) materials as the ferromagnetic layer, propagating spin waves can be excited^{28,29}, offering potential for long-range synchronization³⁰. Moreover, recent advancements have highlighted the potential of SHNOs arrays as tunable nanoscale signal sources, capable of synchronized producing coherent spin-wave interference patterns³¹. The long-range synchronization of SHNOs arrays via spin wave coupling faces significant challenges due to the rapid decay of the amplitude of the propagating spin wave packet in metallic ferromagnets, which is less than 1 μm . Moreover, in spin Hall devices, the effective damping of the ferromagnetic/heavy metal bilayers increases tremendously due to strong spin-orbit coupling^{32–34}; hence, the propagation length shrinks significantly, resulting in an effective synchronization over a distance below 500 nm. Controlling the relative phase between the oscillators represents another fundamental challenge for understanding synchronization in nanoscale devices^{35,36}, where significant progress in phase-resolved techniques has been made to improve accessibility at the nanoscale.

In this work, we study the synchronization of propagating spin waves in a novel spin Hall nano-oscillators (SHNOs) device using micromagnetic simulations. This layout offers two key advantages: (i) the ability to probe the dc current of each oscillator individually, enabling control

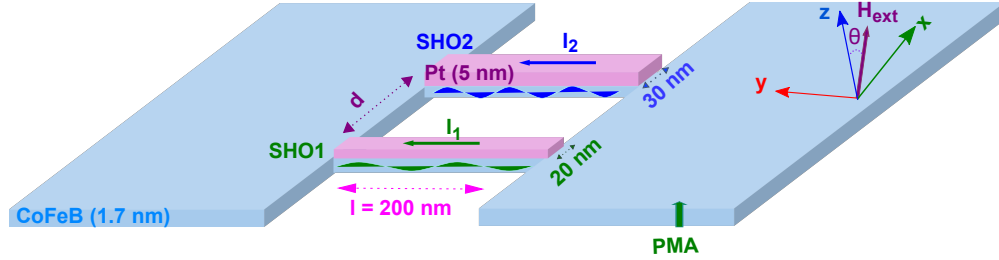


FIG. 1. (Color online) Schematic representation of two nanowire-based Spin Hall oscillators (SHO1 and SHO2). The oscillators consist of a CoFeB (1.7 nm) and Pt (5 nm) bilayer. SHO1 and SHO2 have widths (w) of 20 nm and 30 nm, respectively, a length $l = 200$ nm, and a separation distance d . The schematic also illustrates the direction of the applied external magnetic field and the dc currents I_1 and I_2 .

over the synchronization state, and (ii) direct measurement of the phase of each oscillator. Our results demonstrate that phase locking between two adjacent oscillators occurs when they maintain a constant phase difference, either in-phase or anti-phase, depending on their separation distance.

II. MICROMAGNETIC SIMULATIONS

To initiate micromagnetic simulations, we model a layer comprising 1.7 nm CoFeB patterned rectangular-shaped nanowires of length (l) = 200 nm. The two nanowires oscillators SHO1 and SHO2 have different widths of $w = 20$ and 30 nm, respectively, separated by a distance (d) between 100 and 600 nm as shown in Fig. 1. A 5 nm Pt layer is deposited just over the nanowire with separate connection pads, allowing for an individual control of the current across the two nanowires. In-plane currents of I_1 and I_2 are applied along the y -axis in the 20 nm and 30 nm oscillators, respectively, where a high current density is concentrated within the nanowire region. Micromagnetic simulations were done using the mumax³ solver. In these simulations, we adopt a rectangular mesh with dimensions of $2000 \times 2000 \times 1.7$ nm³ and a cell size of $3.9 \times 3.9 \times 1.7$ nm³. We calculate the electrical current density and the corresponding Oersted field in each oscillator. Then, we convert the electrical current density (J_e) to the spin current density (J_s) via the relation $J_s = \theta_{SH} J_e$, where θ_{SH} represents the spin Hall angle of Pt and is equal to 0.1. Furthermore, in the simulation, we assume that the injected spin current predominantly induces a damping-like torque of the Slonczewski form. For micromagnetic simulations, the CoFeB/Pt nanowires are characterized by a saturation magnetization $\mu_0 M_s$ of 0.9 T, a perpendicular magnetic anisotropy $K_u =$

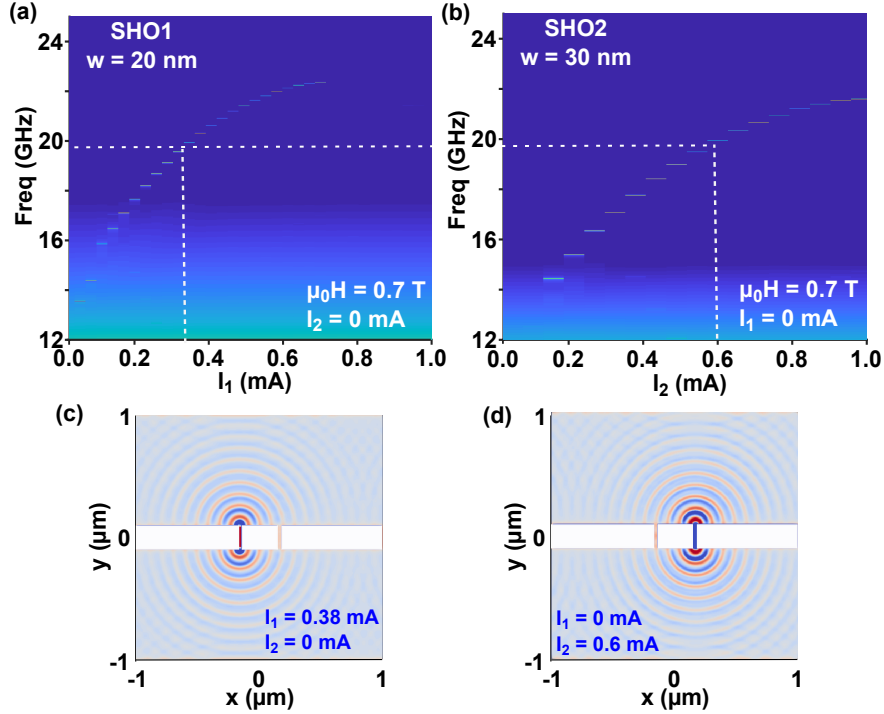


FIG. 2. (Color online) Power spectra color plot of spin-wave modes in (a) SHO1 and (b) SHO2 oscillators as a function of dc current I_1 and I_2 . The white line highlighted the current I_1 and I_2 to generate a frequency of about 19.9 GHz. The micromagnetic simulations were conducted under an applied magnetic field of 0.7 T at an out-of-plane angle of 75° with a perpendicular magnetic anisotropy $K_u = 0.07$ MJ/m³. Two-dimensional snapshots of the magnetization dynamics extracted at (c) ($I_1 = 0.38$ mA, $I_2 = 0$ mA) and (d) ($I_1 = 0$ mA, $I_2 = 0.6$ mA) corresponding to spin wave frequency of 19.95 GHz. Note that the oscillation have identical wavelength of $\lambda = 95$ nm.

0.07 MJ/m³, a gyromagnetic ratio $\gamma/2\pi$ of 30 GHz/T, and an exchange stiffness A of 15 pJ/m, consistent with experimental findings³⁷. A Gilbert damping coefficient α of 0.022 is used in the CoFeB/Pt region, and 0.01 outside. The magnetization dynamics are simulated by integrating the Landau-Lifshits-Gilbert-Slonczewski (LLG-S) equation over 150 ns. Excited mode frequencies and their spatial profiles are determined by performing a Fast Fourier Transform (FFT) of the time-domain data representing magnetization evolution.

III. RESULTS AND DISCUSSION

The proposed layout has the advantage of controlling the injected dc current and reading the induced auto-oscillation characteristics using a spectrum analyzer or the individual phase using an oscilloscope connected to each oscillator experimentally. This device allows for additional tuning of oscillators between synchronized and unsynchronized states. Before analyzing synchronization, we examine the auto-oscillations of each spin Hall oscillator (SHO1 and SHO2) individually. We perform micromagnetic simulations in which the devices are subjected to an external magnetic field applied at 75° out-of-plane of magnitude $\mu_0 H = 0.7$ T. The z -component of the magnetization (m_z) is recorded over time while scanning the applied currents (I_1 in SHO1 or I_2 in SHO2) between 0 and 1 mA. Fig. 2(a) presents the power spectral density of auto-oscillations as a function of I_1 , with I_2 set to 0 mA. The onset current for auto-oscillation excitation is approximately 0.15 mA, with oscillation frequencies ranging from 14 GHz and 23 GHz. Similarly, Fig. 2(b) shows the power spectral density for SHO2 as a function of I_2 , with I_1 set to 0 mA. A continuous auto-oscillation mode is observed, covering the same frequency range. The oscillatory modes in SHO1 and SHO2 correspond to the excitation of propagating spin waves driven by spin torque, exhibiting frequencies higher than the ferromagnetic resonance (FMR) frequency^{28,29}. Due to the different widths of the two oscillators, the wavelengths of the excited spin waves differ; however, these wavelengths can be tuned by adjusting the dc current, as reported in³⁸. For synchronization, both oscillators must oscillate at the same frequency or should have the same wavelength. The mode profiles of the auto-oscillations in SHO1 at $I_1 = 0.38$ mA and in SHO2 at $I_2 = 0.6$ mA are shown in Figs. 2(c) and 2(d). It is observed that propagating spin waves originate at the center of both SHO1 and SHO2 and extend over a considerable distance. Notably, at these current values, the propagating waves exhibit identical wavelengths of approximately 95 nm. As a proof of concept, we will study the synchronization between the oscillators at a frequency of 19.95 GHz, which is achieved at $I_1 = 0.38$ mA and $I_2 = 0.6$ mA.

To investigate the synchronization between the two oscillators, we fix the current I_2 in SHO2 at 0.6 mA, corresponding to a frequency f_2 . In the micromagnetic simulations, we vary the current I_1 in SHO1, leading to the emission of a propagating wave with a tunable frequency f_1 . Figs. 3(a) and 3(b) present a zoomed-in view of the power spectral density as a function of I_1 for two devices with different separation distances between SHO1 and SHO2: 100 nm and 300 nm. The frequency f_2 remains constant, appearing as a continuous line, while f_1 exhibits a nonlinear blue

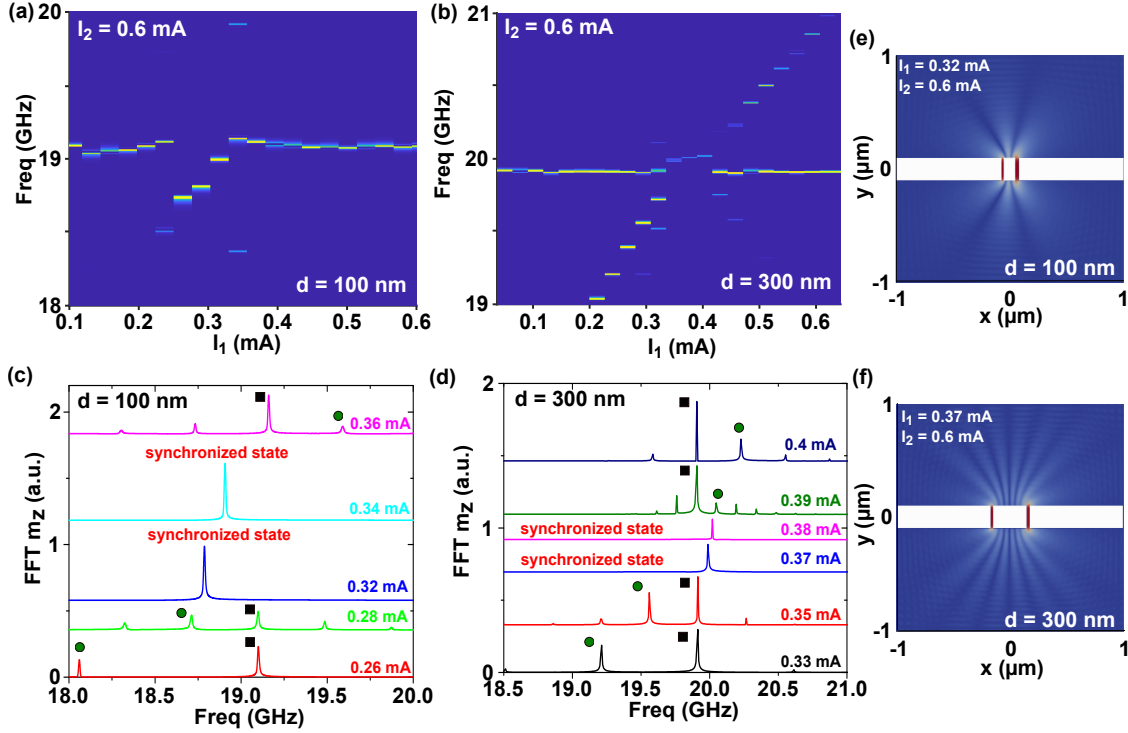


FIG. 3. (Color online)(a, b) Power spectral density color plot of spin-wave modes as a function of the dc current I_1 , calculated at $I_2 = 0.6$ mA, for a separation distance d of (a) 100 nm and (b) 300 nm, demonstrating synchronization between SHO1 and SHO2. (c, d) FFT of m_z as a function of frequency at different I_1 values. The closed square represents the oscillation of SHO2, while the closed circle represents the oscillation of SHO1 for (c) $d = 100$ nm and (d) $d = 300$ nm. (e, f) Spin-wave intensity profiles showing interference patterns for (e) $I_1 = 0.3$ mA and $I_2 = 0.6$ mA, indicating in-phase synchronization, and (f) $I_1 = 0.36$ mA and $I_2 = 0.6$ mA, indicating anti-phase synchronization.

shift with increasing I_1 , consistent with the positive nonlinearity driving the propagating waves. At lower currents, the two STOs oscillate at different frequencies in both devices. As I_1 increases, f_1 gradually approaches f_2 , where we observe a beating effect in m_z over time (not shown). A mutual synchronized state emerges at $I_1 = 0.3$ mA for the 100 nm device [Fig. 3(a)] and at $I_1 = 0.36$ mA for the 300 nm device [Fig. 3(b)]. To confirm synchronization, we analyze the FFT of m_z as a function of frequency, where f_1 and f_2 are highlighted by circles and squares in Figs. 3(c) and 3(d) for $d = 100$ nm and $d = 300$ nm. The frequency spectrum reveals a single dominant frequency within the range $\Delta I_1 = 0.2$ mA, indicating that SHO1 and SHO2 are phase-locked and oscillate coherently at a common frequency, $f_1 = f_2 = f_s$. A key observation is that the nature of

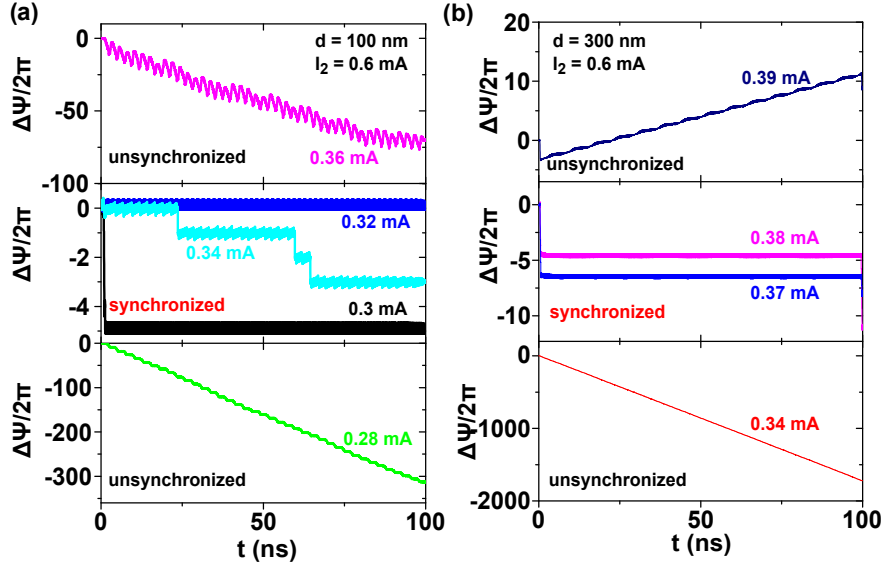


FIG. 4. (Color online) The instantaneous phase difference ($\Delta\Psi$) between SHO1 and SHO2 as a function of time for different values of the direct current I_1 applied to SHO1, for separation distances of (a) 100 nm and (b) 300 nm. The direct current applied to SHO2 is fixed at $I_2 = 0.6$ mA.

the synchronized state differs between the two devices, depending on the separation distance. For $d = 100$ nm, the synchronized frequency is lower than f_2 , whereas for $d = 300$ nm, the synchronized frequency is higher than f_2 . Additionally, synchronization is stronger at shorter separations, leading to a frequency shift of 0.5 GHz and 0.2 GHz for 100 nm and 300 nm separation, respectively. Synchronization in these devices is mediated by spin wave propagation, governed by two key factors. First, the phase difference between the two waves can lead to either in-phase or anti-phase synchronization, manifesting as constructive or destructive interference. Second, the attenuation of the spin-wave amplitude, which decays as $(A \exp(-r/L_{att}))$, with A is the amplitude and L_{att} is the attenuation length, limits synchronization over longer distances, with a cutoff around 600 nm in the present devices. Figs. 3(e) and 3(f) display the spatial intensity profile of the FFT of m_z , revealing the spin wave interference pattern in the synchronized state. For $d = 100$ nm, synchronization occurs in phase, as indicated by a maximum interference pattern at the center between the two oscillators. In contrast, for $d = 300$ nm, synchronization occurs in an anti-phase configuration, with a minimum at the center. These findings demonstrate that the separation distance dictates whether SHO1 and SHO2 synchronize in phase or anti-phase. To gain deeper insight into the synchronization process between the two oscillators, we compute the phase of each oscillator in-

dividually. Using the time traces of m_z , we determine the instantaneous phase difference between the oscillators following the procedure described in³⁹:

$$v_a(t) = v(t) + jH[v(t)] = A(t)e^{\Psi(t)} \quad (1)$$

where j is the imaginary unit, $H[v(t)]$ represents the Hilbert transform of the time trace, $A(t)$ is the instantaneous amplitude, and $\Psi(t)$ is the instantaneous phase of $v(t)$. We independently record the dynamics of each oscillator and extract $\Psi_1(t)$ for SHO1 and $\Psi_2(t)$ for SHO2. Figs. 4(a) and 4(b) present the phase difference $\Delta\Psi(t) = \Psi_1(t) - \Psi_2(t)$ calculated from 100 ns time traces for different values of I_1 in devices with $d = 100$ nm and 300 nm. In theory, phase-locked synchronization requires that the phase difference remains constant over time, i.e., $\Delta\Psi(t) = \Psi_1 - \Psi_2 = \text{constant}$ ¹³. At low currents of I_1 (bottom panel), the instantaneous phase difference varies over time with a negative slope, indicating a fully unsynchronized state. As I_1 increases (central panel), $\Delta\Psi$ stabilizes, signifying a transition from an unsynchronized state to a phase-locked synchronized state. Notably, at transition currents (e.g., for $I_1 = 0.34$ mA), $\Delta\Psi$ exhibits discrete steps over time. Although both oscillators oscillate at the same frequency, their mutual coupling is insufficient to maintain fully locked phase synchronization, leading to periodic desynchronization-resynchronization events over short timescales of approximately 30 ns. Additionally, we observe that synchronization occurs at a random phase difference $\Delta\Psi$ rather than the theoretically expected values of 0 or π . This deviation arises because SHO1 and SHO2 are not identical, leading to an inherent phase offset in their synchronization. At higher current (top panel), the two oscillators oscillate with significantly different phases, leading to an unsynchronized state. This device has several advantages: (i) The local damping is high in the oscillator region, where the propagating wave is initiated, and low outside in the ferromagnet, resulting in larger propagation distances compared to the common spin Hall nano-oscillator layout such as nano-gap or nano-constriction layout. (ii) This layout provides an independent measurement of the phase of the oscillators using, for example, an oscilloscope. Additionally, the fact that two currents can pass through the device offers an extra control parameter for tuning the synchronization process between the two oscillators.

In conclusion, we investigated the synchronization of propagating spin waves in a novel spin-torque oscillator (STO) layout using micromagnetic simulations. This device configuration enables independent probing of the dc current in each oscillator, allowing for precise control of the synchronization state and direct measurement of the oscillator phase. We analyzed the power

spectral density of individual oscillators and identified the conditions under which synchronization occurs. By systematically varying the current in one oscillator while keeping the other fixed, we observed a transition from an unsynchronized state to a phase-locked state. The frequency locking was accompanied by characteristic interference patterns in the spin-wave intensity, confirming the role of propagating spin waves in mediating synchronization. Furthermore, phase analysis revealed that the instantaneous phase difference remains constant in the synchronized state. Our findings provide valuable insights into the synchronization mechanisms of spin Hall nano-oscillator and highlight the influence of separation distance on phase relationships. This work paves the way for further experimental validation and the development of spin-torque based technologies for neuro-morphic computing, frequency generation, and energy-efficient spintronic devices.

ACKNOWLEDGMENTS

This work is supported by the American University of Beirut Research Board (URB).

DATA AVAILABILITY

The data that support the findings of this study are available from the corresponding author upon reasonable request.

REFERENCES

- ¹J. A. Acebron, L. L. Bonilla, C. J. P. Vicente, F. Ritort, and R. Spigler, “The Kuramoto model: A simple paradigm for synchronization phenomena,” *Rev. Mod. Phys.* **77** (2005).
- ²A. Slavin and V. Tiberkevich, “Nonlinear auto-oscillator theory of microwave generation by spin-polarized current,” *IEEE Transactions on Magnetics* **45**, 1875–1918 (2009).
- ³V. E. Demidov, S. Urazhdin, and S. O. Demokritov, “Direct observation and mapping of spin waves emitted by spin-torque nano-oscillators,” *Nat. Mater.* **9**, 984–988 (2010).
- ⁴A. Slavin and V. Tiberkevich, “Spin wave mode excited by spin-polarized current in a magnetic nanocontact is a standing self-localized wave bullet,” *Phys. Rev. Lett.* **95**, 237201 (2005).
- ⁵A. Houshang, R. Khymyn, H. Fulara, A. Gangwar, M. Haidar, S. R. Etesami, R. Ferreira, P. P. Freitas, M. Dvornik, R. K. Dumas, and J. Åkerman, “Spin transfer torque driven higher-order propagating spin waves in nano-contact magnetic tunnel junctions,” *Nature Communications* **9**, 4374 (2018).

- ⁶M. Haidar, A. Awad, M. Dvornik, R. Khymyn, A. Houshang, and J. Åkerman, “A single layer spin-orbit torque nano-oscillator,” *Nature Communications* **10**, 2362 (2019).
- ⁷M. Torrejon, J. Riou, F. A. Araujo, S. Tsunegi, G. Khalsa, D. Querlioz, P. Bortolotti, V. Cros, K. Yakushiji, A. Fukushima, H. Kubota, S. Yuasa, M. D. Stiles, and J. Grollier, “Neuromorphic computing with nanoscale spintronic oscillators,” *Nature* **547**, 428–431 (2017).
- ⁸S. Tsunegi, T. Taniguchi, K. Nakajima, S. Miwa, K. Yakushiji, A. Fukushima, S. Yuasa, and H. Kubota, “Physical reservoir computing based on spin torque oscillator with forced synchronization,” *Applied Physics Letters* **114**, 164101 (2019), https://pubs.aip.org/aip/apl/article-pdf/doi/10.1063/1.5081797/14525804/164101_1_online.pdf.
- ⁹M. Romera, P. Talatchian, S. Tsunegi, F. Abreu Araujo, V. Cros, P. Bortolotti, J. Trastoy, K. Yakushiji, A. Fukushima, H. Kubota, S. Yuasa, M. Ernoult, D. Vodenicarevic, T. Hirtzlin, N. Locatelli, D. Querlioz, and J. Grollier, “Vowel recognition with four coupled spin-torque nano-oscillators,” *Nature* **563**, 230–234 (2018).
- ¹⁰B. Dieny, I. L. Prejbeanu, K. Garello, P. Gambardella, P. Freitas, R. Lehndorff, W. Raberg, U. Ebels, S. O. Demokritov, J. Åkerman, A. Deac, P. Pirro, C. Adelman, A. Anane, A. V. Chumak, A. Hirohata, S. Mangin, S. O. Valenzuela, M. C. Onbaşlı, M. d’Aquino, G. Prenat, G. Finocchio, L. Lopez-Diaz, R. Chantrell, O. Chubykalo-Fesenko, and P. Bortolotti, “Opportunities and challenges for spintronics in the microelectronics industry,” *Nature Electronics* **3**, 446 (2020).
- ¹¹F. B. Mancoff, N. D. Rizzo, B. N. Engel, and S. Tehrani, “Phase-locking in double-point-contact spin-transfer devices,” *Nature* **437**, 393–395 (2005).
- ¹²M. R. Pufall, W. H. Rippard, S. E. Russek, S. Kaka, and J. A. Katine, “Electrical measurement of spin-wave interactions of proximate spin transfer nanooscillators,” *Phys. Rev. Lett.* **97**, 087206 (2006).
- ¹³A. N. Slavin and V. S. Tiberkevich, “Theory of mutual phase locking of spin-torque nanosized oscillators,” *Phys. Rev. B* **74**, 104401 (2006).
- ¹⁴D. V. Berkov, “Synchronization of spin-torque-driven nano-oscillators for point contacts on a quasi-one-dimensional nanowire: Micromagnetic simulations,” *Phys. Rev. B* **87**, 014406 (2013).
- ¹⁵S. Erokhin and D. Berkov, “Robust synchronization of an arbitrary number of spin-torque-driven vortex nano-oscillators,” *Phys. Rev. B* **89**, 144421 (2014).
- ¹⁶M. A. Castro, D. Mancilla-Almonacid, B. Dieny, S. Allende, L. D. Buda-Prejbeanu, and U. Ebels, “Mutual synchronization of spin-torque oscillators within a ring array,” *Scientific Re-*

- ports **12**, 12030 (2022).
- ¹⁷L. Martins, A. S. Jenkins, J. Borme, J. Ventura, P. P. Freitas, and R. Ferreira, “Second harmonic injection locking of coupled spin torque vortex oscillators with an individual phase access,” *Communications Physics* **6**, 72 (2023).
- ¹⁸M. Madami, S. Bonetti, G. Consolo, S. Tacchi, G. Carlotti, G. Gubbiotti, F. B. Mancoff, M. A. Yar, and J. Åkerman, “Direct observation of a propagating spin wave induced by spin-transfer torque,” *Nat. Nanotechnol.* **6**, 635–638 (2011).
- ¹⁹T. Kendziorczyk, S. O. Demokritov, and T. Kuhn, “Spin-wave-mediated mutual synchronization of spin-torque nano-oscillators: A micromagnetic study of multistable phase locking,” *Phys. Rev. B* **90**, 054414 (2014).
- ²⁰A. Houshang, E. Iacocca, P. Dürrenfeld, S. R. Sani, J. Åkerman, and R. K. Dumas, “Spin-wave-beam driven synchronization of nanocontact spin-torque oscillators,” *Nature Communications* **9**, 4374 (2018).
- ²¹T. Kendziorczyk and T. Kuhn, “Mutual synchronization of nanoconstriction-based spin hall nano-oscillators through evanescent and propagating spin waves,” *Phys. Rev. B* **93**, 134413 (2016).
- ²²R. Lebrun, S. Tsunegi, P. Bortolotti, H. Kubota, A. S. Jenkins, M. Romera, K. Yakushiji, A. Fukushima, J. Grollier, S. Yuasa, and V. Cros, “Mutual synchronization of spin torque nano-oscillators through a long-range and tunable electrical coupling scheme,” *Nature Communications* **8**, 15825 (2017).
- ²³T. Taniguchi, S. Tsunegi, and H. Kubota, “Mutual synchronization of spin-torque oscillators consisting of perpendicularly magnetized free layers and in-plane magnetized pinned layers,” *Applied Physics Express* **11**, 013005 (2017).
- ²⁴A. Houshang, M. Zahedinejad, S. Muralidhar, J. Chęciński, R. Khymyn, M. Rajabali, H. Fulara, A. A. Awad, M. Dvornik, and J. Åkerman, “Phase-binarized spin hall nano-oscillator arrays: Towards spin hall ising machines,” *Phys. Rev. Appl.* **17**, 014003 (2022).
- ²⁵A. Litvinenko, R. Khymyn, V. H. González, R. Ovcharov, A. A. Awad, V. Tyberkevych, A. Slavin, and J. Åkerman, “A spinwave ising machine,” *Communications Physics* **6**, 227 (2023).
- ²⁶A. A. Awad, P. Dürrenfeld, A. Houshang, M. Dvornik, E. Iacocca, R. K. Dumas, and J. Åkerman, “Long-range mutual synchronization of spin hall nano-oscillators,” *Nat. Phys.* **13**, 292–299 (2017).
- ²⁷M. Zahedinejad, A. A. Awad, S. Muralidhar, R. Khymyn, H. Fulara, H. Mazraati, M. Dvornik,

- and J. Åkerman, “Two-dimensional mutually synchronized spin hall nano-oscillator arrays for neuromorphic computing,” *Nature nanotechnology* **15**, 47 (2020).
- ²⁸H. Fulara, M. Zahedinejad, R. Khymyn, A. A. Awad, S. Muralidhar, M. Dvornik, and J. Åkerman, “Spin-orbit torque–driven propagating spin waves,” *Science Advances* **5** (2019), 10.1126/sciadv.aax8467.
- ²⁹M. Succar and M. Haidar, “Spin wave excitations in a nanowire spin hall oscillator with perpendicular magnetic anisotropy,” *J. Appl. Phys.* **133**, 093901 (2023).
- ³⁰A. Kumar, A. K. Chaurasiya, V. H. González, N. Behera, A. Alemán, R. Khymyn, A. A. Awad, and J. Åkerman, “Spin-wave-mediated mutual synchronization and phase tuning in spin hall nano-oscillators,” *Nat. Phys.* **21**, 245–252 (2025).
- ³¹M. Haidar, “Interference patterns of propagating spin wave in spin-Hall oscillator arrays,” *Journal of Applied Physics* **135**, 223901 (2024), https://pubs.aip.org/aip/jap/article-pdf/doi/10.1063/5.0209653/19997379/223901_1_5.0209653.pdf.
- ³²M. Ranjbar, P. Dürrenfeld, M. Haidar, E. Iacocca, M. Balinskiy, T. Q. Le, M. Fazlali, A. Houshang, A. Awad, R. Dumas, and J. Åkerman, “CoFeB-based spin hall nano-oscillators,” *IEEE Magn. Lett.* **5**, 3000504 (2014).
- ³³Y. Yin, F. Pan, M. Ahlberg, M. Ranjbar, P. Dürrenfeld, A. Houshang, M. Haidar, L. Bergqvist, Y. Zhai, R. K. Dumas, A. Delin, and J. Åkerman, “Tunable permalloy-based films for magnonic devices,” *Phys. Rev. B* **92**, 024427 (2015).
- ³⁴M. Haidar, H. Mazraati, P. Dürrenfeld, H. Fulara, R. M., and J. Åkerman, “Compositional effect on auto-oscillation behavior of ni100–xfex/pt spin hall nano-oscillators,” *Appl. Phys. Lett.* **118**, 012406 (2021).
- ³⁵A. Slavin, “Spin-torque oscillators get in phase,” *Nature nanotechnology* **4**, 479–480 (2009).
- ³⁶A. Ruotolo, V. Cros, B. Georges, A. Dussaux, J. Grollier, C. Deranlot, R. Guillemet, K. Bouzehouane, S. Fusil, and A. Fert, “Phase-locking of magnetic vortices mediated by antivortices,” *Nature nanotechnology* **4**, 528–532 (2009).
- ³⁷M. Zahedinejad, H. Mazraati, H. Fulara, J. Yue, S. Jiang, A. A. Awad, and J. Åkerman, “CMOS compatible W/CoFeB/MgO spin Hall nano-oscillators with wide frequency tunability,” *Appl. Phys. Lett.* **112**, 132404 (2018).
- ³⁸M. Haidar, “Short spin waves excitation in spin hall nano-oscillators,” *Journal of Magnetism and Magnetic Materials* **587**, 171336 (2023).
- ³⁹L. Bianchini, S. Cornelissen, J.-V. Kim, T. Devolder, W. van Roy, L. Lagae, and C. Chap-

Synchronization of propagating spin waves in spin Hall oscillators: A micromagnetic study

pert, “Direct experimental measurement of phase-amplitude coupling in spin torque oscillators,” *Applied Physics Letters* **97**, 032502 (2010), https://pubs.aip.org/aip/apl/article-pdf/doi/10.1063/1.3467043/14436648/032502_1_online.pdf.